IOP Conference Series: Earth and Environmental Science

PAPER • OPEN ACCESS

Reconstruction of the spring-summer precipitation on the Southern Ural

To cite this article: D Y Vasiliev *et al* 2020 *IOP Conf. Ser.: Earth Environ. Sci.* **606** 012064

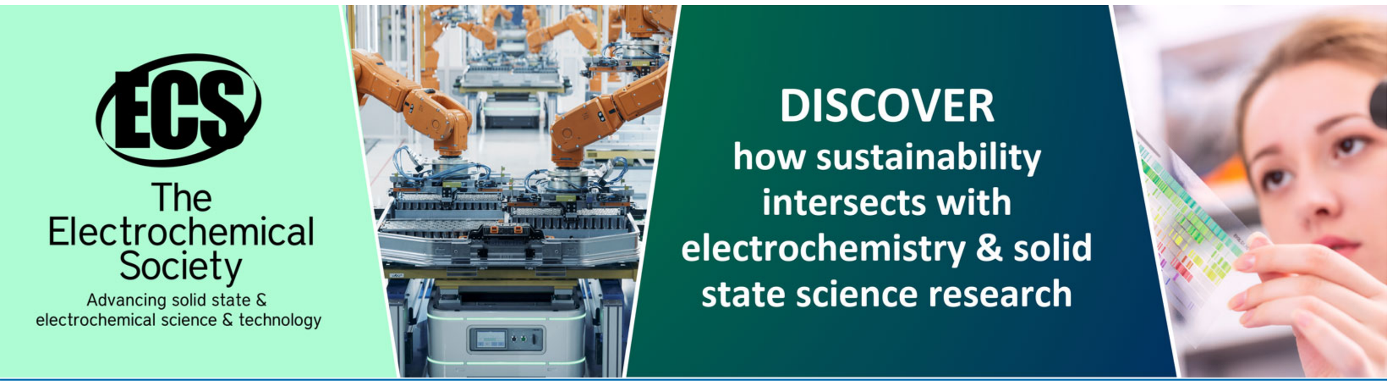

Reconstruction of the spring-summer precipitation on the Southern Ural

D Y Vasiliev [1,2], V A Semenov [2,3], S E Kucherov[4]

[1] Ufa State Aviation Technical University, Ufa, 450008 Russia
[2] A.M. Obukhov Institute of Atmospheric Physics Russian Academy of Science, Moscow 119017 Russia
[3] Institute of Geography Russian Academy of Science, Moscow, 119017 Russia
[4] Ufa Institute of Biology Russian Academy of Science, Ufa, 450054 Russia

vasilevdy@ugatu.su vasemenov@ifaran.ru skucherov@mail.ru

Abstract. The article present a reconstruction of the late spring–summer (May–July) precipitation for the Zilair plateau (Southern Urals) based on latewood width chronologies of Scots pine (*Pinus sylvestris* L.) for the 1776–2015 period. Wavelet analysis revealed a number of characteristic periodicities in the reconstructed precipitation variability. Cross-wavelet analysis using indices of solar activity (SA), Atlantic Multidecadal Oscillation (AMO) and North Atlantic Oscillation (NAO) showed co-variability of the precipitation with SA at about 20-yr, sporadic links to NAO on multi-year to decadal time scale, and a robust link to AMO at multidecadal time scales.

1. Introduction

To extend the length of the rainfall time series in the past, reconstruction methods based on various proxy data including tree rings, corals, stalactites-stalagmites, ice cores and others have been typically used. Recently, the number of publications on the reconstruction of precipitation in different regions of the world have increased significantly [1–12]. This approach in particular made it possible to create a grid archive of reconstructed seasonal precipitation for Europe that spans more than 500 years [13].

Studies on the variability of precipitation are particularly important at the regional level in moisture-limited areas, which include the forest-steppe part of the Southern Urals and the western piedmont of the Ural Mountains. The current paper presents the results of the reconstruction of the May-July precipitation based on the analysis of the Scots pine radial growth in the region of the Zilair plateau (Southern Urals).

2. Data and Methods

The area under investigation belongs to the central part of the Zilair plateau located in the South Urals. The climate of the Zilair plateau is continental. According to the weather station Zilair (52.2°N, 57.4°E), the average for the 1933-2012 period annual temperature is +1.9 °C and the average annual rainfall is 550 mm.

Samples of common pine wood (*Pinus sylvestris* L.) were taken from three sites, (ZL1, ZL2, SR) (Fig. 1). ZL1 (52 ° 13.2′ N, 57 ° 26.3′ E, elevation is 460-490 m above sea level) and ZL2 (52 ° 13.7′ N, 57 ° 25.5 ′ E, 470-480 m above sea level) are located in the midstream area of the Zilair river near the Zilair village. On the ZL1 site, pines grow on the northwestern slope with a steepness of 15-60 degrees to the Zilair river. The height of the pines is 19–23 m, the diameter is 22–44 cm, and the life span is up to 260 years. On the ZL2 site, pines grow on the eastern and southeastern slopes with a steepness of 5-50 degrees to the Zilair river. The height of the pines is 14–20 m, the diameter is 34–80 cm, and the life span is up to 260 years. The SR site (52 ° 20′ N, 57 ° 12–14′ E, 510–520 m above sea level) is located in the upstream area of the Big Suren river. Here, pines grow as solitary trees together with larch (*Larix sukaczewii* Dyl.), as well as along the edges of a deciduous forest (*Quercus robur* L., *Tilia cordata* L.); the height of the trees is 15–24 m, the diameter is 36–70 cm, and the life span is up to 250 years.

Core samples were extracted from trees at heights of 0.2–1.0 m from ground level using an increment borer. The measurements of the sample's ring width (RW) and the width of the latewood (LW) zone were conducted. Dating of ring width was carried out visually before measurements on the base of using pointer year layers [14]. In total, the data of the measurements using 53 trees from site SR, 33 trees from site ZL1 and 15 trees from site ZL2 were analyzed in the this study.

Instrumental data that included the sum of monthly precipitation for 1933–2012 and average monthly temperatures for 1936–2012 were taken from the Zilair weather station, located 20 km south-east from the site SR, and 1.5–2 km from the sites ZL1 and ZL2. The solar activity data based on sunspot numbers were taken from the Solar Influences Data Analysis Center - SIDC (http://sidc.oma.be/sunspot-data/), with an observation period of 1700-2012. The data on climatic indices AMO (1856-2012) and NAO (1865-2012) were taken from the Climate Data Guide (http://climatedataguide.ucar.edu/).

3. Results and Discussion

The climate–growth relationships were investigated using correlation analysis between tree-ring chronologies and meteorological data with the DendroClim software. The correlation was calculated for periods beginning in May for the year preceding the growth and ended in the September of the growth year, and considered separately for the first and second parts of the period and for the entire span of the meteorological data. The statistical confidence of the regression model was examined using split period calibration–verification tests. Calibration and verification were carried out in two steps. In the first step, calibration was carried out for the primary interval of the meteorological data, whereas verification was performed for the second part of the interval based on calibration equation derived from the treatment of the primary. For the second step, the reverse procedure was used when calibration was made for the second interval of the meteorological data and verification was performed for the first interval. Verification of the calibration equations for an independent part of the data was performed using correlation analysis, the statistical indicator RE (reduction of error), and the sign test. A statistically significant positive correlation (p-value is about 0.05) for both RW and LW chronologies was obtained for the precipitation in May, June and July of the current year in both parts of the meteorological observation period (figure 1). The correlation is stronger for the LW chronology. The strongest correlation for LW chronology ($r = 0.78$, $p < 0.01$) was obtained for the total precipitation in May – July.

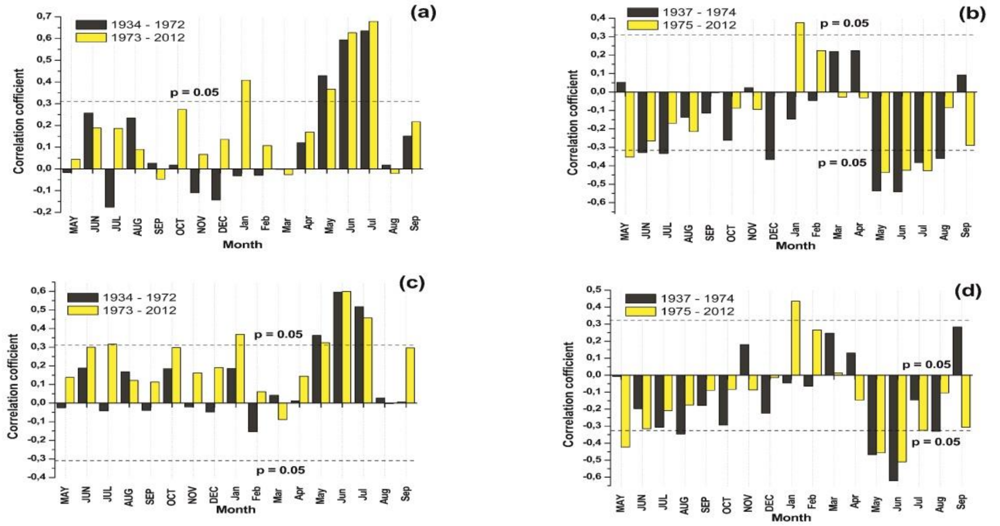

Figure 1. Correlations of LW and RW chronologies with precipitation and temperature records: **a**, **b** are for LW, whereas **c** and **d** are for RW chronologies. Horizontal dashed lines denote significant level.

Based on the established strong correlation between the LW chronology of pine with precipitation in current May, June and July, a regression model was built by means of calibration of LW chronology for the May–July precipitation. The split-period verification consisted of calibrating the model for the 1933–1972 period and verification for the 1973–2012 period followed by calibrating the model for 1973–2012 and verification for the 1933–1972 period. From the combined interval, the final calibration equation was constructed as the following:

$$Precipitation_{(V-VII)} = 111.453LW(t) + 50.126, \quad (1)$$

where, $\text{precipitation}_{(\text{V-VII})}$ – reconstructed data of precipitation in May-July, LW(t) – the width of the late wood, and the values of coefficients of the regression equation.

This model accounted for 60% of the actual precipitation variance. The correlation coefficient between real and calculated May – July precipitation over 1933–2012 was found to be 0.78 with a synchronism of 87%. The standard deviation of observed precipitation was 1.5-fold larger than for the calculated one. Smoothing the precipitation time series with a 10-year spline increased the correlation coefficient to 0.81 and decreased the standard deviations down to 1.35. This indicates that the model better describes precipitation variability on a decadal time scale.

Based on the obtained regression model linking May–July precipitation with the LW growth, reconstruction of the May–July precipitation from 1776 to the current time was carried out and is presented in Figure 2.

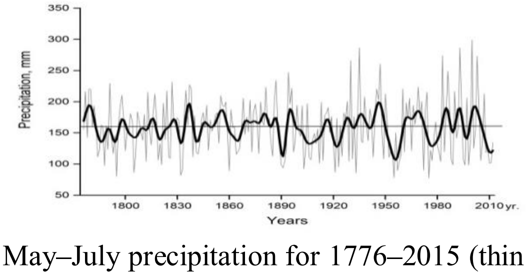

Figure 2. Reconstruction of May–July precipitation for 1776–2015 (thin grey curve), its average (thin horizontal line) and its 10–year smoothing spline (thick black curve).

The reconstructed May-July precipitation variability is representative for a rather large region within 50N-55N and 45E-65E. Spatial correlation between reconstructed and instrumental May-July precipitation data during 1950-2015 period showed highest correlation coefficients (r >0.7) for the Urals and Trans-Urals regions (Figure3).

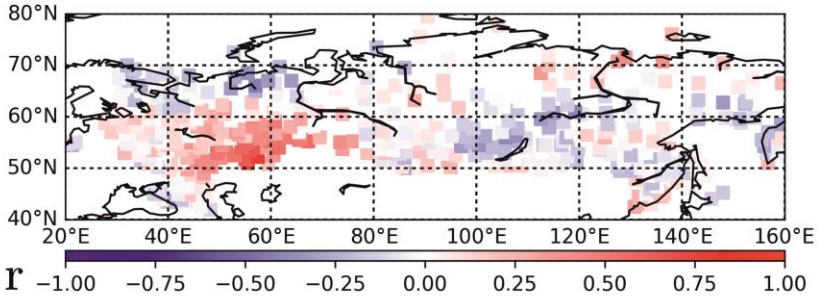

Figure 3. Spatial correlations between the May–July precipitation reconstruction and the observed data set (http://www.meteo.ru/) for the 1950–2015 period. r – Pearson correlation coefficient.

Figure 4 shows the results of spectral analysis performed by the wavelet transform method for the precipitation reconstruction (Figure 4a), sunspot numbers (Figure 4b), Atlantic Multidecadal Oscillation (AMO) (Figure 4c) and North Atlantic Oscillation (NAO) (Figure 4d) indices.

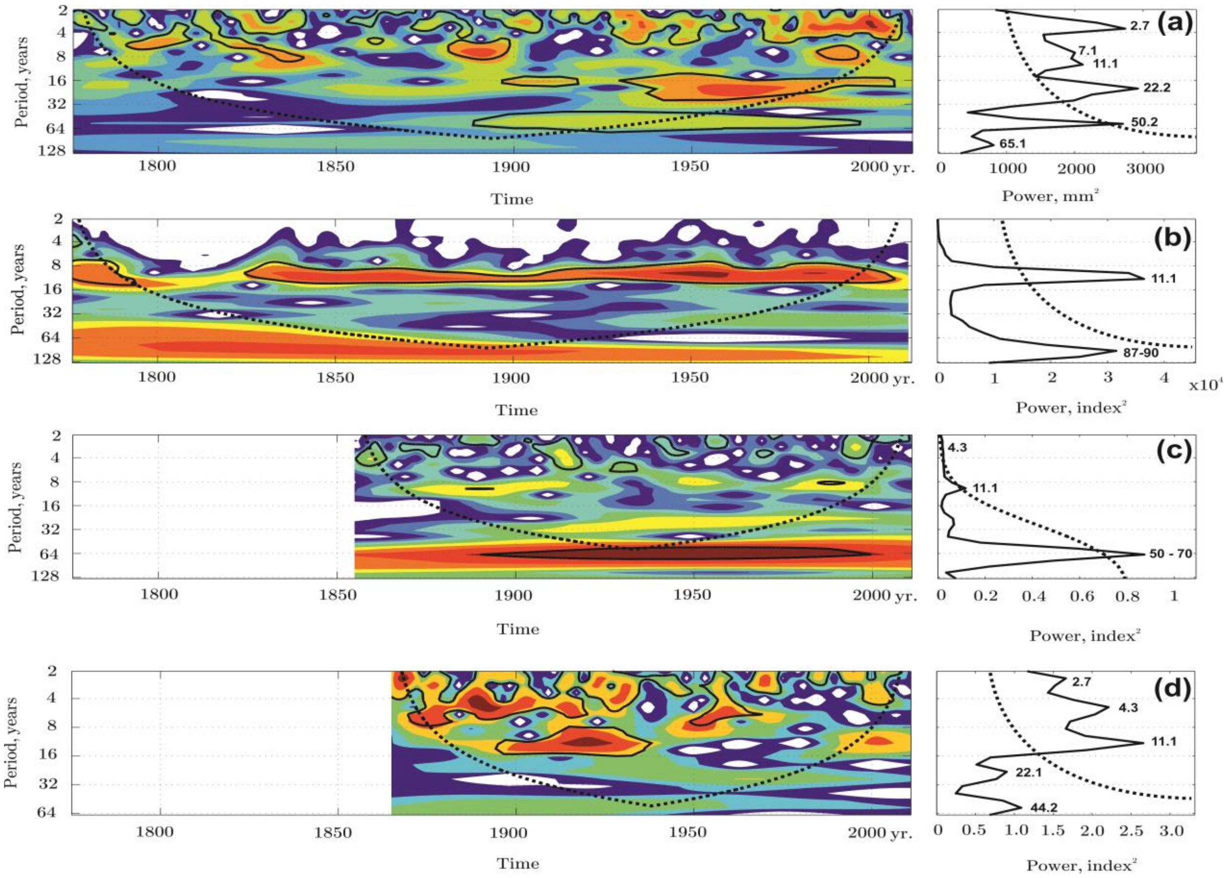

Figure 4. Local wavelet spectrum: (a) wavelet analysis results of precipitation reconstruction time series, (b) SSN, (c) AMO and (d) NAO indices. The dash line indicates 95% confidence level.

The determined with the wavelet transform method cycles of precipitation and climate indices can be tentatively divided into two groups: sub-decadal oscillations with periods from 2.7 to 7.1 years and low-frequency oscillations with a period of 11 years or longer. It is clear from figure 4 that cycles with the periods of 2.7–7.1 years are characteristic only for the reconstructed precipitation and AMO and NAO climate indices, whereas they are not present in the solar activity data. Variations with durations of 11 years and longer are found in the analyzed precipitation data and all climate indices considered. Figure 4 suggests that contribution of the low-frequency fluctuations is dominant in the precipitation time series, indicating the importance of climatic factors for the precipitation variability in the considered region. The peaks at 11.1 and 22.2 yr are well consistent with the 11-y cycle of Solar activity, and those at 2.7 yr. fall within the range of inter-annual variability of the Quasi-biennial Oscillation (QBO).

To estimate a strength of co-variability of the reconstructed precipitation at different time scales with solar activity (SSN), AMO and NAO indices, a cross-wavelet analysis was carried out. A cross-wavelet analysis of reconstructed precipitation data and SSN revealed a predominantly in-phase coherence of oscillations localized in the region of low-frequency (quasi-eleven-year) fluctuations. The cross-wavelet analysis with NAO index showed a statistically significant antiphase coupling in the high-frequency (2–7 years) and the low-frequency (11 and 22 years) domains together with a common co-variability mode in the low-frequency region with a duration of 40 years and longer. CWT of the precipitation series with AMO index revealed a statistically significant relationship in the low-frequency region at the end of the 19th century, with an in-phase of 22 years and out-of-phase coherences for about 60 year period.

4. Conclusions

The ring-width data-set used in this study comprised 101 living trees and was compiled from material sampled across a large part of the Zilair plateau to maximize the large-scale common signal while minimizing the site specific, ecological and management effects. The strongest climate-growth response was found with May–July precipitation (r = 0.78) over the 1933–2012 calibration period. Based on the chronology of the growth of late wood from *Pinus sylvestris*, the reconstruction of May – July precipitation for the 1776–2015 period was carried out. The reconstruction explains 60 % of the instrumental May–July rainfall variance and, in particular, reflects well the droughts, which were known from either meteorological records or reported in available archival materials and publications. It also shows a reasonably good agreement with a few precipitation reconstructions in nearby regions. A comparison of wet and dry spells showed that long wet spells are present in the first half of the reconstruction - at the end of the 18th and 19th centuries, whereas dry spells dominate in the second half of the reconstruction, in the late 19th, early and 1950s of the 20th and early 21st centuries. The deepest minima in the smoothed (by 10-year spline) reconstructed record were determined for the end of 1880-s and beginning of 1890s, as well as for the 1950s and at the end of the first and beginning of the second decades of the 21st century.

Quasi-periodicities of 2.7 yr., 7.1 yr., 11.1 yr., 22.2 yr., 50.2 yr. and 65.1 yr. were detectable, with the 65.1 yr. quasiperiodicitie being more no significant statistically. These interannual variations are intermittent and may correlate with the regional hydroclimatic variability over different time intervals with changing phase. The periods of coherent and in-phase variability of precipitation have not been reported earlier from this region. Increased (decreased) proportion of frontal precipitation offers a plausible explanation for enhanced (faded) coherence at the interannual timescale in large scale hydroclimate signal. These results emphasize the great potential of proxy climate data, owing to their longer span, to contribute novel information impossible to retrieve otherwise from shorter instrumental observation records. These findings, however, not only corroborate the earlier assertion that neither the strength nor the rank of similarity of the local hydroclimate signals is stable throughout the past centuries in East Europe but also contribute to the explanation of the more localized information of the hydroclimate proxy records in the region. A cross-wavelet analysis of the reconstructed precipitation with the climate and solar activity indices revealed some noticeable links. A co-variability was found with sunspot number at about 20-yr period, sporadic links to NAO on

IOP Conf. Series: Earth and Environmental Science **606** (2020) 012064 doi:10.1088/1755-1315/606/1/012064

multi-year to decadal time scale, and a robust link to AMO at multidecadal time scales were detected. In general, the found links were stronger with NAO and AMO than with SSN.

Acknowledgments
The analysis of climate variability and links was supported by the Ministry of Science and Higher Education within the framework of the State Assignment under contract No. 0148-2019-0009, data collection and reconstruction was supported by the Ministry of Science and Higher Education, contract No 075–00326–19–00.

References
[1] Büntgen U, Tegel W, Nicolussi K, McCormick M, Frank D, Trouet V, Kaplan J, Herzig F, Heussner U, Wanner H, Luterbacher J, Esper J 2011 *Science* **331** 578–582
[2] Chen Z, Zhang X, Cui M, He X, Ding W, Peng J 2012 *Global and Planetary Change* **86/87** 45–56.
[3] Chen F; Yuan Y.J; Wei W.S; Zhang R.B, Yu S.L, Shang H.M, Zhang T.W, Qin L, Wang H.Q, Chen F.H 2013 *Boreas* **42** 1008–1021
[4] Cooper R.J, Melvin T.M, Tyers I, Wilson R.J.S, Briffa K.R 2013 *Climate Dyn*. **3–4** 1019–1039
[5] Griggs C, Pearson C, Manning S.W, Lorentzen B 2014 *Int. J. Climatol*. **34** 2702–2714
[6] Kucherov S.E, Vasil'ev D.Yu., Muldashev A.A 2016 *Russian Journal of Ecology* **47** 115–124
[7] Land A, Remmele S, Hofmann J, Reichle D, Eppli M, Zang C, Buras A, Hein S, and Reiner Zimmermann 2019 *Clim. Past* **15** 1677–1690
[8] Linderholm H.W, Nicolle M, Francus P, Gajewski K, Helama S, Korhola A, Solomina O, Yu Z, Zhang P, D'Andrea W.J, Debret M, Divine D.V, Gunnarson B.E, Loader N.J, Massei N, Seftigen K, Thomas E.K, Werner J, Andersson S, Berntsson A, Luoto T.P, Nevalainen L, Saarni S, Väliranta M 2018 *Clim. Past.* **14** 473–514
[9] Lopez L, Stahle D, Villalba R, Torbenson M, Feng S, Cook E 2017 *Geophys. Res. Lett*. **44** 7410–7418
[10] Vasil'ev D.Yu, Kucherov S.E, Lazarev V.V 2016 *Atmospheric and Oceanic Optics* **29** 224–231
[11] Wilson R.J.S, Miles D, Loader N.J, Melvin T, Cunningham L, Cooper R, Briffa K 2013 *Clim. Dyn*. **40** 997–1017
[12] Zhang T, Zhang R, Yuan Y, Gao Y, Wei W, Diushen M, He Q, Shang H, Wang J 2015 *Quaternary International* **358** 58–67
[13] Pauling A, Luterbacher J, Carlo Casty C, Heinz Wanner H 2006 *Climate Dynamics* **26** 387–405
[14] Schlesinger M.E, Ramankutty N 1994 *Nature* **367** 723–726